Supplements of:
Importance of forest states in estimating biomass loss from tropical forests: combining individual-based forest models and remote sensing

Ulrike Hiltner[1,2,3], Andreas Huth[1,4,5], Rico Fischer[1]

[1]Department of Ecological Modelling, Helmholtz-Centre for Environmental Research GmbH - UFZ, 04318 Leipzig, Germany

[2]Institute of Geography, Friedrich-Alexander-University Erlangen-Nuremberg, Erlangen, 91058, Germany

[3]Department Environmental System Sciences, ETH Zurich, 8092 Zurich, Switzerland

[4] German Centre for Integrative Biodiversity Research – iDiv Halle-Jena-Leipzig, 04103 Leipzig, Germany

[5] Institute for Environmental Systems Research, University Osnabruck, 49076 Osnabruck, Germany

Correspondence to: Ulrike Hiltner (u.hiltner.uh@gmail.com)

1 Tables

Table S1: In FORMIND we used allometric relationships to calculate the geometry of each tree. Functional relations at tree level used in this study with aboveground biomass *(AGB)*, crown diameter (*cd*), stem circumference (*circ*), crown length *(cl)*, stem diameter at breast height *(dbh)*, stem diameter increment (*dinc)*, form factor (*f)*, growth height (*h)*, leaf area index (*LAI)*, tree mortality rate (*m)*, wood density (ρ), fraction of stem biomass to total aboveground biomass (*tr)*. Further basic functions are listed in Fischer et al. (2016).

Geometric relation at tree level	**Function**
stem circumference-dbh	$dbh(circ) = circ/\pi$
aboveground biomass-dbh	$agb(dbh) = \pi/4 * \rho/tr * dbh^2 * h * f$
crown diameter-dbh	$cd(dbh) = cd_0 * dbh^{cd_1}$
crown length-height	$cl(h) = cl_0 * h$
stem diameter increment-dbh	$dinc(dbh) = a_0 * dbh * (1 - dbh/dbh_{max}) * exp(-a_1 * dbh)$
form factor-dbh	$f(dbh) = f_0 * dbh^{f_1}$
tree height-dbh	$h(dbh) = h_0 * dbh/(h_1 + dbh)$
leaf area index-dbh	$lai(dbh) = l_0 * dbh^{l_1}$
mortality-dbh	$m(dbh) = m_0 * e^{-m_1 * dbh}$

Table S2: The PFT-specific parameter values used in the baseline scenario to simulate forests with the forest model FORMIND, the meaning of the parameters, and unit used for the Paracou site. For detailed information about the parameterization process please see Hiltner et al., (2018).

Parameter	Description	Unit	PFT1	PFT2	PFT3	PFT4	PFT5	PFT6	PFT7	PFT8	Reference
Light and establishment											
k	light extinction coefficient	-	0.7	0.7	0.7	0.7	0.7	0.7	0.7	0.7	(Köhler et al., 2003)
n_{seed}	global number of seeds	1 ha^{-1}	2	27	2	15	14	16	20	2	(Hiltner et al., 2018)
i_{seed}	Minimum light intensity to establish	-	0.01	0.01	0.05	0.20	0.01	0.02	0.15	0.01	(Köhler et al., 2003)
Geometry											
h_{max}	maximum growth height	m	16.50	34.22	34.61	34.85	40.40	39.96	38.58	39.06	(Hiltner et al., 2018)
h_0	height-dbh-relation	-	47.0	47.0	47.0	47.0	47.0	47.0	47.0	47.0	(Hiltner et al., 2018)
h_1	height-dbh-relation	-	0.276	0.276	0.276	0.276	0.276	0.276	0.276	0.276	(Hiltner et al., 2018)
cd_0	crown diameter-dbh-relation	-	13.12	13.12	13.12	13.12	13.12	13.12	13.12	13.12	(Hiltner et al., 2018)
cd_1	crown diameter-dbh-relation	-	0.59	0.59	0.59	0.59	0.59	0.59	0.59	0.59	(Hiltner et al., 2018)
l_0	LAI-dbh-relation	-	2.0	2.0	2.0	2.0	2.0	2.0	2.0	2.0	(Hiltner et al., 2018)
l_1	LAI-dbh-relation	-	0.0	0.0	0.0	0.0	0.0	0.0	0.0	0.0	(Hiltner et al., 2018)
f_0	form factor-dbh-relation	-	0.425	0.425	0.425	0.425	0.425	0.425	0.425	0.425	(Hiltner et al., 2018)
f_1	form factor-dbh-relation	-	-0.18	-0.18	-0.18	-0.18	-0.18	-0.18	-0.18	-0.18	(Fischer et al., 2014)
cl_0	crown length factor-height-relation	-	0.358	0.358	0.358	0.358	0.358	0.358	0.358	0.358	(Köhler et al., 2003)

σ	fraction of stem biomass-total biomass	-	0.7	0.7	0.7	0.7	0.7	0.7	0.7	0.7	(Hiltner et al., 2018)
Biomass and productivity											
ρ	wood density	$t_{odm} * m^{-3}$	0.76	0.77	0.66	0.55	0.83	0.73	0.56	0.62	calculated from (Chave et al., 2009; Zanne et al., 2009)
M	transmission coefficient of leafs	-	0.1	0.1	0.1	0.1	0.1	0.1	0.1	0.1	(Larcher, 1994)
r_g	Growth respiration	-	0.2	0.2	0.2	0.2	0.2	0.2	0.2	0.2	(Ryan, 1991)
α	slope of light response curve	$\mu mol_{CO_2} * \mu mol_{photons}^{-1}$	0.043	0.043	0.035	0.086	0.043	0.043	0.086	0.043	(Köhler et al., 2003); (Hiltner et al., 2018)
p_{max}	maximum leaf photosynthesis	$\mu mol_{CO_2} * (m^2 * s)^{-1}$	1.12	0.55	2.00	20.59	1.35	1.50	27.00	1.46	(Hiltner et al., 2018)
g_{max}	maximum annual stem diameter increment	m/a	0.011	0.018	0.017	0.014	0.025	0.013	0.022	0.031	(Hiltner et al., 2018)
g_{DBHmax}	maximum stem diameter	-	0.24	0.17	0.12	0.11	0.30	0.11	0.17	0.37	(Hiltner et al., 2018)
Mortality											
M_n	background mortality rate	-	0.01	0.01	0.013	0.02	0.01	0.01	0.02	0.01	(Hiltner et al., 2018)
fallP	probability of dead tree to fall	-	0.5	0.5	0.5	0.5	0.5	0.5	0.5	0.5	(Hiltner et al., 2018)
Management- module											
$comm_{spec}$	proportion of commercially logged species	-	0.0	0.0362	0.2393	0.0865	0.5718	0.5531	0.3311	0.2706	(Hiltner et al., 2018)
log_{DBH}	dbh lower cutting threshold	m	0.55	0.55	0.55	0.55	0.55	0.55	0.55	0.55	(Hiltner et al., 2018)

Site-specific climate				
I_S	Mean annual irradiance above canopy	$\mu mol_{photons}/(m^2 * s)^{-1}$	694.0	(Köhler et al., 2003)
D_L	Length of daily photosynthetic active period	h	12	(Huth and Ditzer, 2000)

Table S3: Comparison of multiple linear regression model fits with biomass loss (mAGB) as explanatory variable and multiple forest attributes as proxy variables, such as forest height (H), leaf area index (LAI), biomass (AGB), gross primary production (GPP), and net primary production (NPP). The intercepts of the equations were set to 0 because we assumed that there is no forest when the forest attributes are 0. The robust standard errors of the proxy variables are shown in parentheses and the p-value is *** < 0.01, ** < 0.05, and * < 0.1, β: coefficients).

Model type	β_H	β_{LAI}	β_{AGB}	β_{GPP}	β_{NPP}	adjusted R^2	RMSE
1 (cf. Eq. 7)	0.004166*** (4.5e-5)	-0.030614*** (44.9e-5)				0.9467	0.0099
2	0.001143*** (1.1e-5)					0.8281	0.0179
3		0.010728*** (14.4e-5)				0.7260	0.0227
4			8.4e-5*** (0.2e-5)			0.5969	0.0275
5				0.000814*** (1.4e-5)		0.6285	0.0264
6					0.003295*** (4.6e-5)	0.7078	0.0234
7			3.9e-5*** (0.3e-5)	0.000502*** (2.4e-5)		0.6658	0.0250
8			-1.7e-5*** (0.4e-5)		0.003864*** (13.5e-5)	0.7104	0.0233
9	0.002514*** (2.3e-5)		-0.000124*** (0.2e-5)			0.9396	0.0106
10		0.041005*** (54.6e-5)	-0.000266*** (0.5e-5)			0.8908	0.0143
11		0.008674*** (30.2e-5)		0.00019*** (2.5e-5)		0.7335	0.0223
12		0.007971*** (62.8e-5)			0.000881*** (19.5e-5)	0.7285	0.0225
13	0.001888*** (4.2e-5)				-0.002403*** (13.0e-5)	0.8521	0.0166
14	0.00116*** (2.4e-5)			-1.6e-5 (1.9e-5)		0.8281	0.0179
15				5.1e-5 (3.4e-5)	0.003112*** (13.0e-5)	0.7080	0.0234

2 Figures

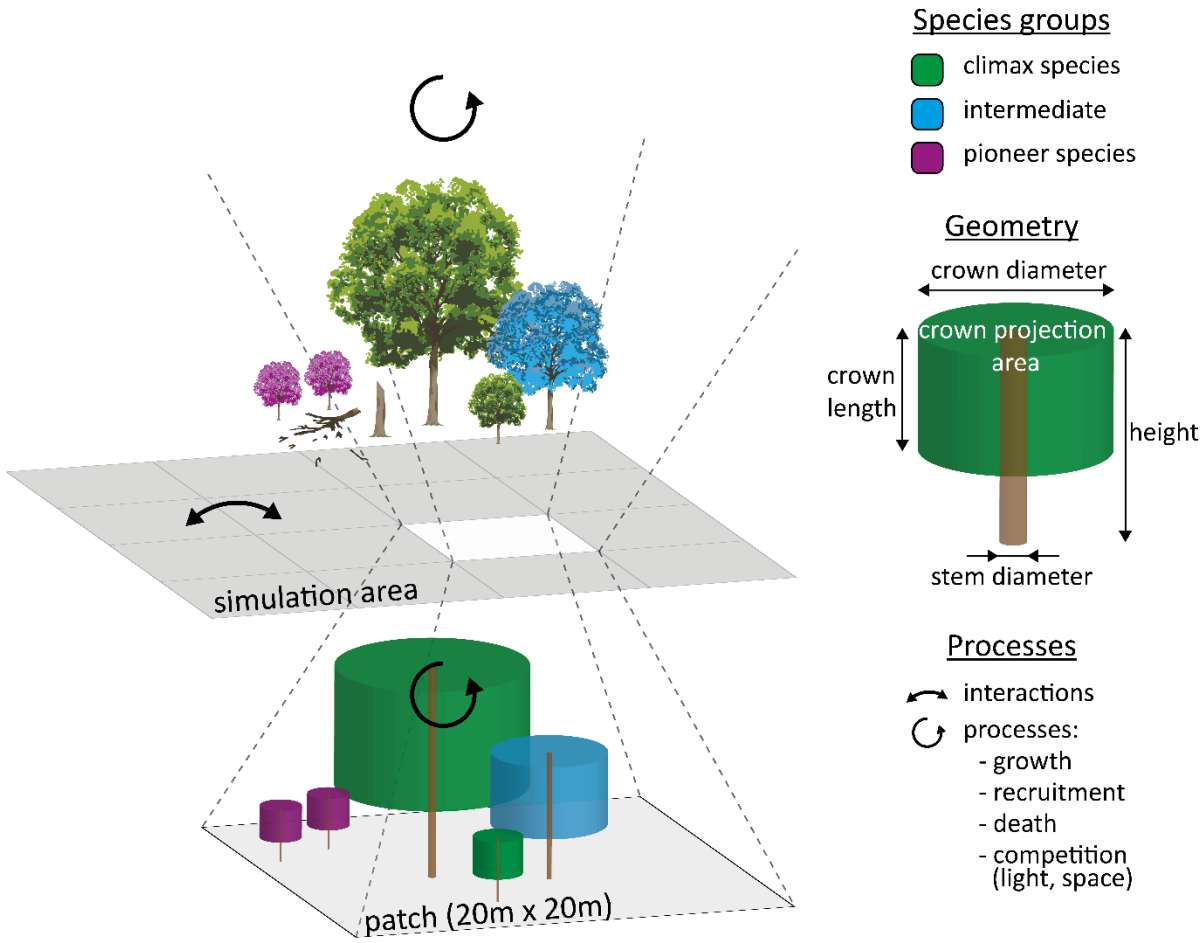

Figure S1: FORMIND belongs to the family of forest gap models. Trees compete for resources at the patch level (20 m ·20 m). FORMIND is an individual-based forest model, where the growth of every tree is simulated. The main processes considered are tree growth, competition for light and space, regeneration, and mortality. Since tropical forests are species-rich, tree species are grouped into plant functional types (PFTs) according to functional traits, such as potential stem diameter increment rates (for more details see Hiltner et al., 2018; Fischer et al., 2016). In this study, the total simulation area is 16 hectares consisting of one-hectare forest stands that grow on interacting patches. The temporal resolution of the simulations is one year.

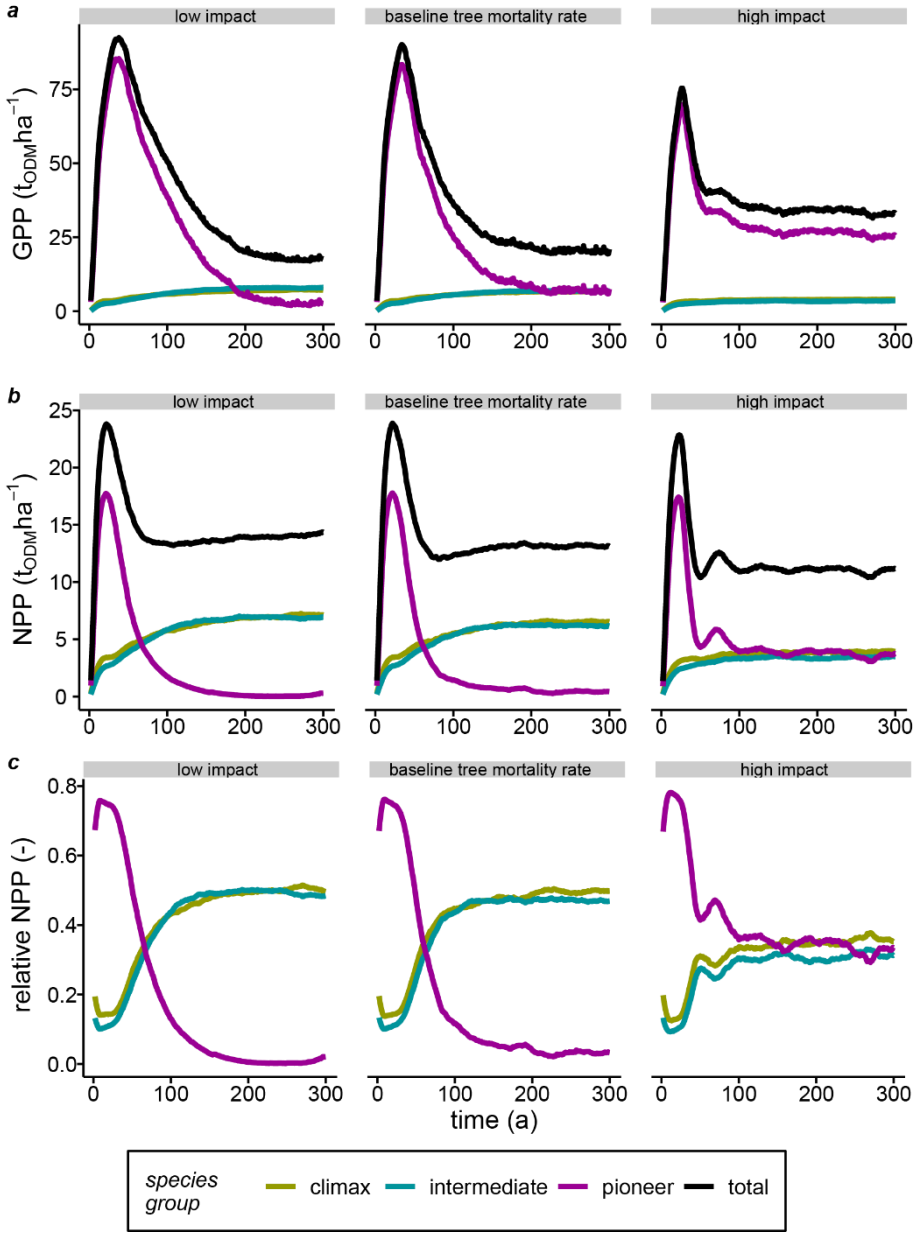

Figure S2: Simulation results of (a) gross primary production (GPP), (b) net primary production (NPP), and (c) relative NPP (i.e., proportion of PFT-specific NPP to stand NPP) for three species groups for terra firme forests in French Guiana (low impact: tree mortality intensity of 0.32%, baseline: tree mortality intensity of 1.29%, high impact: tree mortality intensity of 5.16%, ODM: organic dry matter).

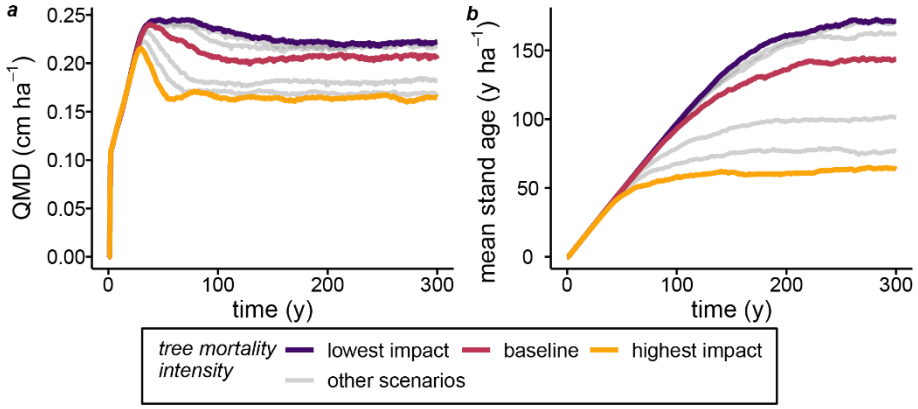

Figure S3: Development of (a) quadratic mean diameter (QMD) and (b) mean stand age of simulated terra firme forest stands for different tree mortality intensities. Grey lines indicate the entire set of scenarios under varying tree mortality rates (eq. 1). (QMD: Square root of the sum of squared stem diameters per tree divided by the number of trees in a stand, mean stand age: arithmetic mean age of the 25 oldest trees per simulated 1 ha area (selection of the oldest tree per patch, see Fig. S1), ODM: organic dry matter).

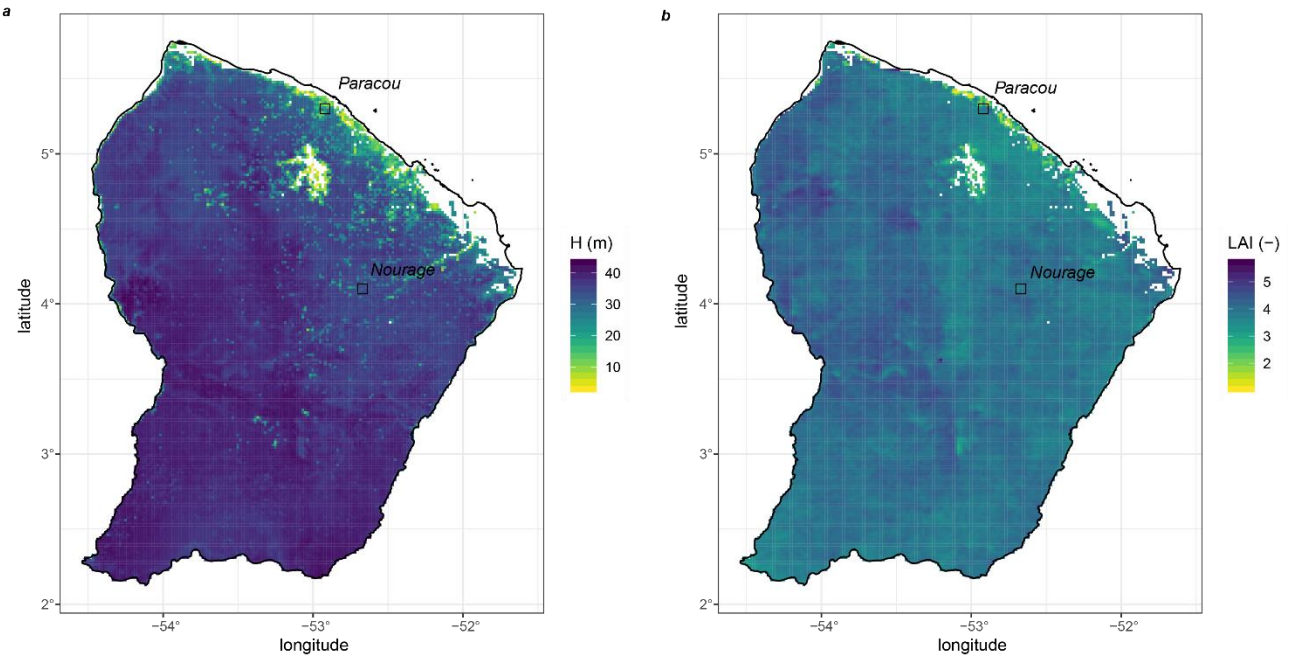

Figure S4: Input data used for deriving a biomass loss map for French Guiana (~ 2 km resolution). (a) 'Simard' map of forest height (H; 1 km resolution; Simard et al., 2011) and (b) map of the LAI derived from MODIS (MCD15A2H Version 6, resolution 500 m). 139 MODIS LAI values were averaged between 2004-01-31 and 2006-12-31 (Myneni et al., 2015; LAI: leaf area index).

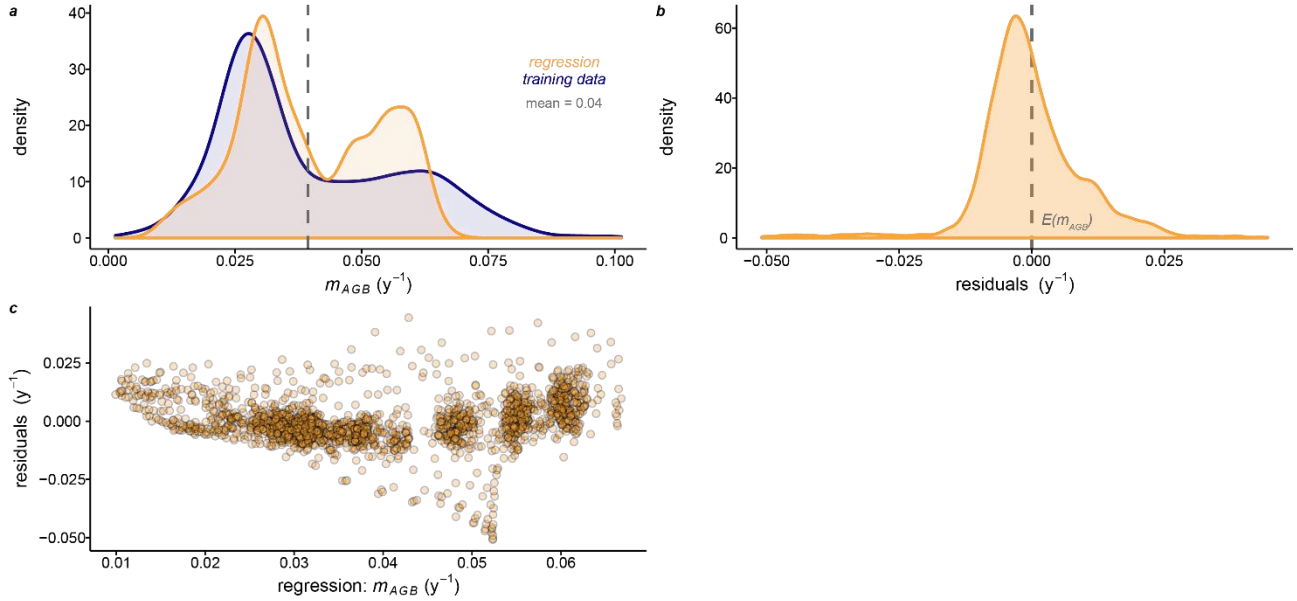

Figure S5: Analysis of the derived regression model (eq. 7; Tab. S3). (a) Frequency distributions of simulated training data versus biomass loss rates (m_{AGB}) derived from the multiple linear regression model. The dashed lines indicate the arithmetic means of both distributions. (b) Test for normally distributed residuals of m_{AGB} around the expectation value ($E(m_{AGB})$) indicated by the dashed line. (c) Test for homoscedasticity of the residuals over fitted m_{AGB}.

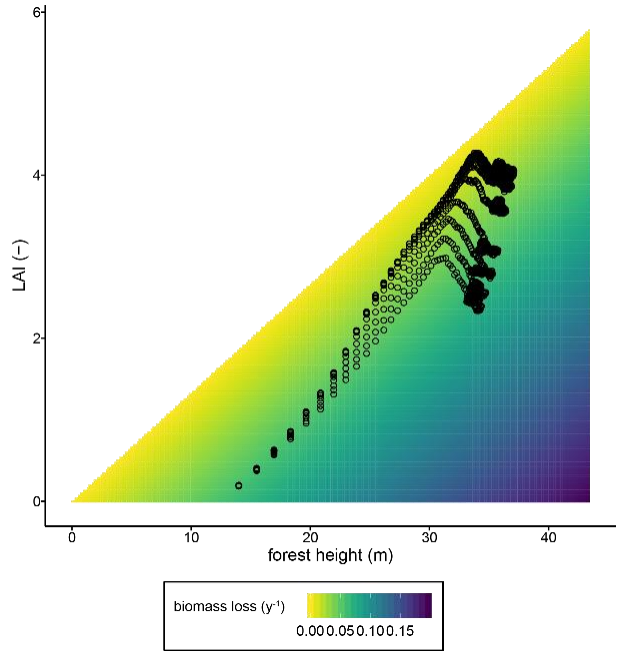

Figure S6: Heat map of biomass loss rates based on the derived multiple linear regression model (eq. 6, Tab. S3) for different LAI and forest height values. Black dots represent the simulation data of terra firme forest stands used to fit the multiple linear regression model which (LAI: leaf area index).

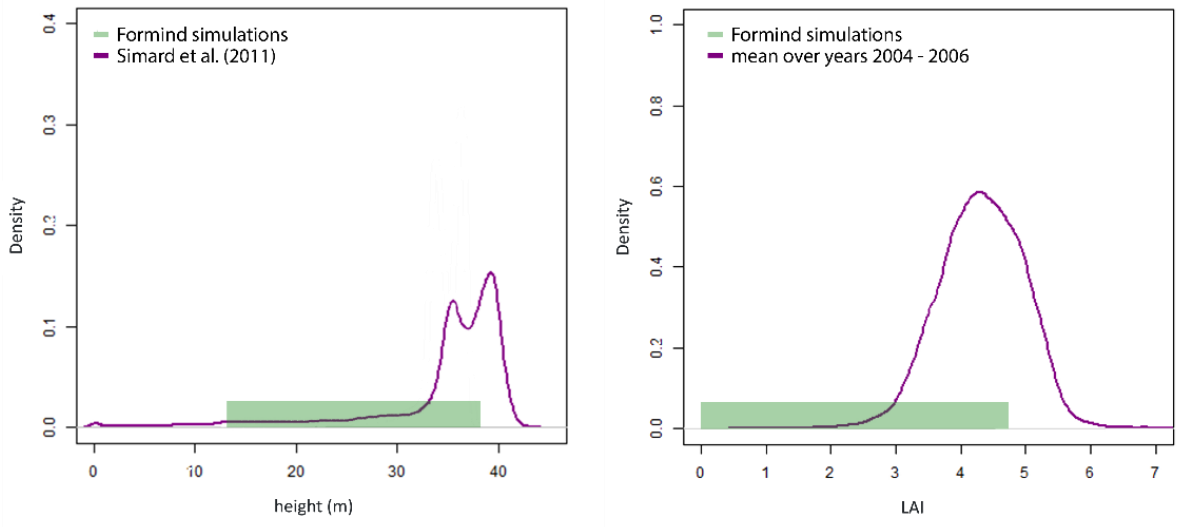

Figure S7: Comparison of simulation results and remote sensing products. Density distributions for the (a) forest height and (b) leaf area index (LAI) (remote sensing products see Fig. S4). Green bars show the range of obtained values of the forest simulations.

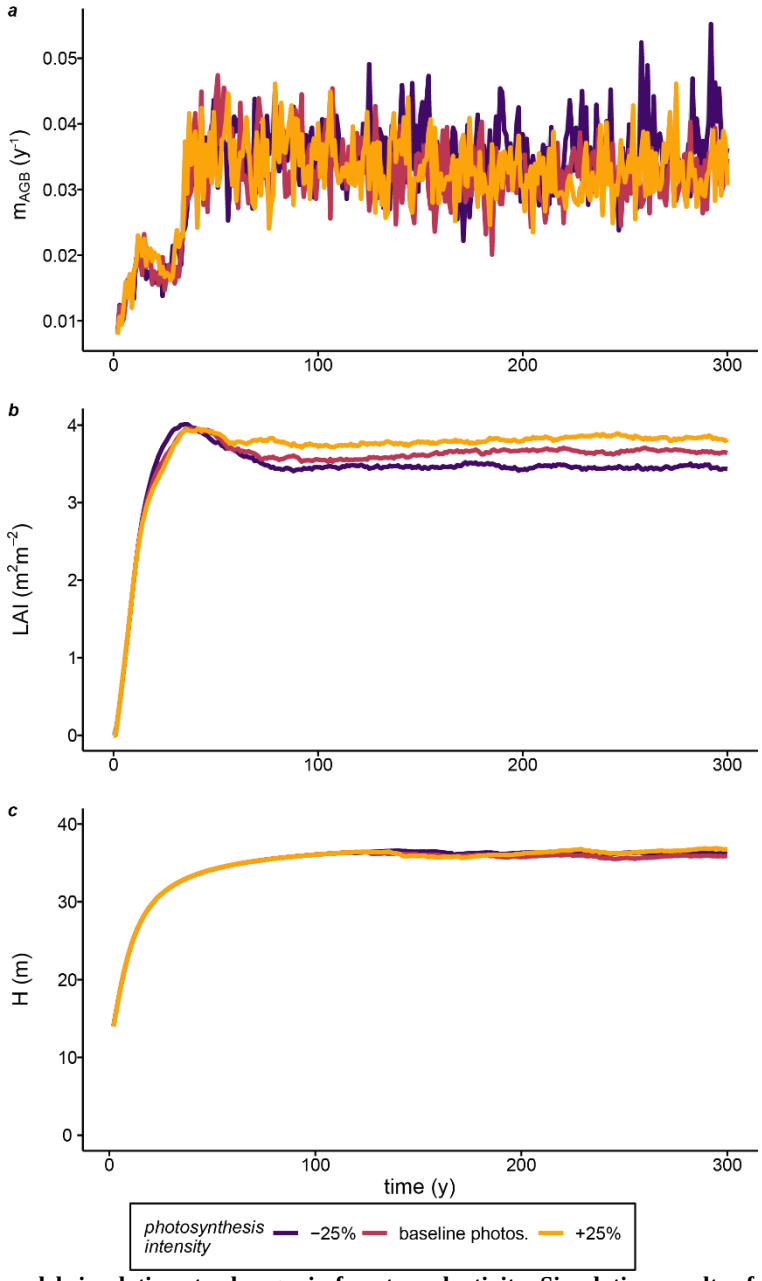

Figure S8: Sensitivity of the model simulations to changes in forest productivity. Simulation results of (a) the biomass loss (m_{AGB}), (b) leaf area index (LAI), and (c) forest height (H) for different levels of photosynthesis (±25%, starting from the baseline scenario). All test scenarios produce results showing similar ranges compared the simulation results of the scenarios with the varying tree mortality intensities (cf. Fig. 3.a, 3.c, 3.d). This means our multiple linear regression model (eq. 7) is robust to local changes in photosynthesis. The tree related parameters of the potential photosynthetic rates (pmax) of each PFT (p) of the reference scenario (bl) was multiplied by a factor (f) per scenario (sc) ($pmax_{p,sc} = f \cdot pmax_{p,bl}$, with f = {0.75, 1.25}).

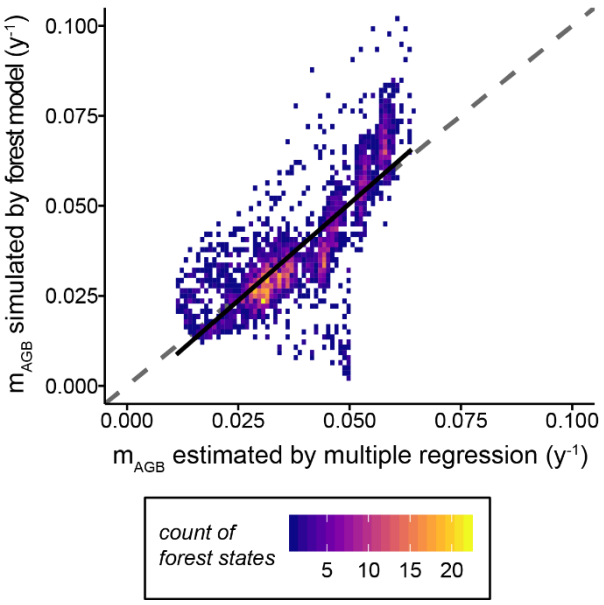

Figure S9: Sensitivity of the multiple linear regression model to changes in forest productivity. 1:1-plot of biomass loss (m_{AGB}) values simulated by the forest model versus the estimated ones using a regression model with forest height and leaf area index as proxy variables. Here, the simulated data includes scenarios of varying rates of tree mortality and also the scenarios of the changed forest productivity (see eq. 1 and Fig S8). The dashed line shows the 1:1-line. Each dot represents a forest stand with a unique forest structure (i.e., tree size distribution and functional species composition) while colours show the density distribution of the combinations. The black solid line indicates the mean deviation of the simulated biomass loss from the estimated ones. For the alternative multiple linear regression model, we obtained: m_{AGB} = 0.0039 H - 0.0284 L + ε (R^2 = 0.9414; RMSE = 0.01; p-value = 0; m_{AGB}: rate of biomass loss due to tree mortality, L: leaf area index, H: forest height, ε: error term). With respect to coefficients and regression statistics, this differs only little from the previous regression model (eq. 6, Table 2). The comparison of biomass loss rates for more than 33600 forest stands estimated by the multiple linear regression model (cf. eq. 6; Tab. 2) versus that of the simulated ones fit well (linear regression statistics of black solid line: $m_{AGB,DFM} = 1.0776 \cdot m_{AGB,LM} - 0.0033 + \varepsilon$, R^2 = 0.6297, RMSE = 0.01, p-value = 0).

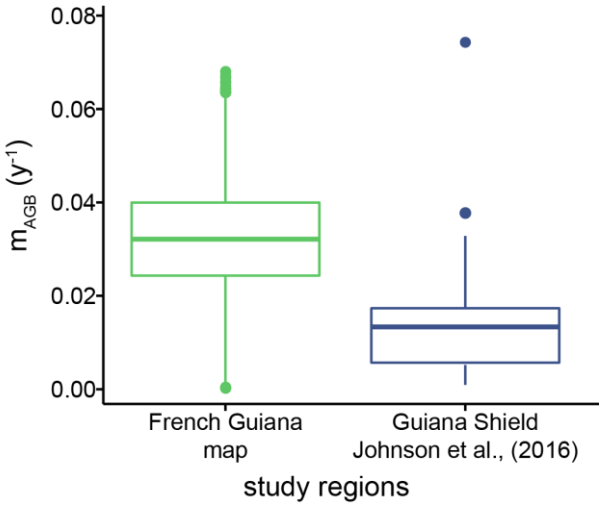

Figure S10: Comparison of biomass loss (m_{AGB}) obtained for French Guiana (map, cf. Fig. 7) with census-based values for the entire Guiana Shield (i.e., French Guiana, Suriname, Guyana, northern Brazil, eastern Venezuela; Johnson et al., 2016). Please note, Johnson et al. (2016) estimated biomass mortalities across the entire Guiana Shield, with higher values in French Guiana.

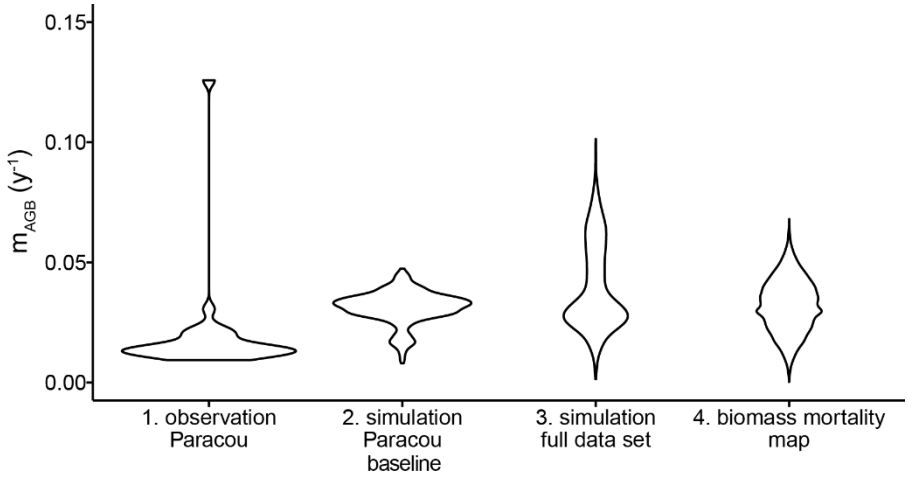

Figure S11: Comparison of frequency distributions for the biomass loss (m_{AGB}) across different data sources (used in this study). The (1.) census-based biomass loss for Paracou's T0-plots and T1-plots (see Hiltner et al., 2018), the simulation results (2.) of the baseline scenario (including different succession states, simulation years 0-300), and (3.) of the full set of all simulation scenarios (baseline scenario and scenarios including different tree mortality intensities, simulation years 0-300), and (4.) the results for the estimated biomass loss map.

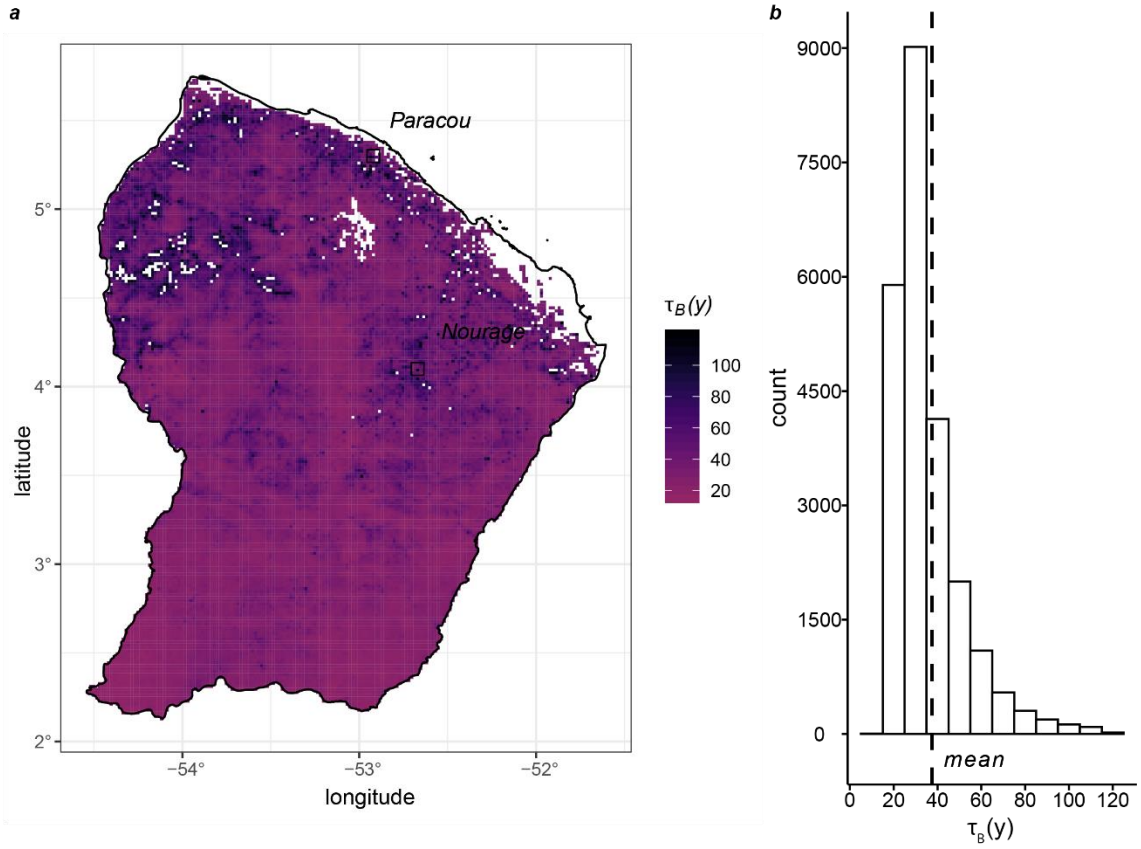

Figure S12: (a) Map of biomass turnover time distribution of simulated terra firme forests in French Guiana (~2-km resolution) and (b) the histogram. The dashed line in b) indicates the estimated country-wide mean (35 y, standard deviation of 15 y). The leaf area index and forest height were used as proxy variables. The black squares in the map show the locations of forest plots at Paracou and Nourage, of which census-data was used to compare estimated and field-based biomass loss values (Projection: WGS-84, EPSG: 4326, τ_B: biomass turnover time (eq. 5)).

3 Software used

To process the simulation data of FORMIND v3.2 as well as the forest height map and LAI map (Myneni et al., 2015; Simard et al., 2011), version 3.6.2 of the R statistical software (R Core Team, 2019) with the packages 'tidyverse' v1.2.1 (Wickham et al., 2019), ‘viridis’ (Garnier, 2018), ‘broom’ (Robinson and Hayes, 2020), ‘ggpubr’ (Kassambara, 2020), ‘data.table’ (Dowle and Srinivasan, 2019), ‘gdalUtils’ (Greenberg and Mattiuzzi, 2020), ‘rgeos’ (Bivand and Rundel, 2019), and ‘raster’ (Hijmans, 2020) were used. The FORMIND forest model can be downloaded for free at www.formind.org.

4 References

Bivand, R. and Rundel, C.: rgeos: Interface to Geometry Engine - Open Source ('GEOS'), [online] Available from: https://cran.r-project.org/package=rgeos, 2019.

Chave, J., Coomes, D., Jansen, S., Lewis, S. L., Swenson, N. G. and Zanne, A. E.: Towards a worldwide wood economics spectrum, Ecol. Lett., 12(4), 351–366, doi:10.1111/j.1461-0248.2009.01285.x, 2009.

Dowle, M. and Srinivasan, A.: data.table: Extension of `data.frame`, [online] Available from: https://cran.r-project.org/package=data.table, 2019.

Fischer, R., Armstrong, A., Shugart, H. H. and Huth, A.: Simulating the impacts of reduced rainfall on carbon stocks and net ecosystem exchange in a tropical forest, Environ. Model. Softw., 52, 200–206, doi:10.1016/j.envsoft.2013.10.026, 2014.

Garnier, S.: viridis: Default Color Maps from "matplotlib," [online] Available from: https://cran.r-project.org/package=viridis, 2018.

Greenberg, J. A. and Mattiuzzi, M.: gdalUtils: Wrappers for the Geospatial Data Abstraction Library (GDAL) Utilities, [online] Available from: https://cran.r-project.org/package=gdalUtils, 2020.

Hijmans, R. J.: raster: Geographic Data Analysis and Modeling, [online] Available from: https://cran.r-project.org/package=raster, 2020.

Hiltner, U., Bräuning, A., Huth, A., Fischer, R. and Hérault, B.: Simulation of succession in a neotropical forest: High selective logging intensities prolong the recovery times of ecosystem functions, For. Ecol. Manage. [online] Available from: https://www.sciencedirect.com/science/article/pii/S0378112718311964, 2018.

Huth, A. and Ditzer, T.: Simulation of the growth of a lowland Dipterocarp rain forest with FORMIX3, Ecol. Modell., 134(1), 1–25, doi:10.1016/S0304-3800(00)00328-8, 2000.

Jucker, T., Caspersen, J., Chave, J., Antin, C., Barbier, N., Bongers, F., Dalponte, M., van Ewijk, K. Y., Forrester, D. I., Haeni, M., Higgins, S. I., Holdaway, R. J., Iida, Y., Lorimer, C., Marshall, P. L., Momo, S., Moncrieff, G. R., Ploton, P., Poorter, L., Rahman, K. A., Schlund, M., Sonké, B., Sterck, F. J., Trugman, A. T., Usoltsev, V. A., Vanderwel, M. C., Waldner, P., Wedeux, B. M. M., Wirth, C., Wöll, H., Woods, M., Xiang, W., Zimmermann, N. E. and Coomes, D. A.: Allometric equations for integrating remote sensing imagery into forest monitoring programmes, Glob. Chang. Biol., 23(1), 177–190, doi:10.1111/gcb.13388, 2017.

Kassambara, A.: ggpubr: "ggplot2" Based Publication Ready Plots, [online] Available from: https://cran.r-project.org/package=ggpubr, 2020.

Köhler, P., Chave, J., Riéra, B. and Huth, A.: Simulating the long-term response of tropical wet forests to fragmentation, Ecosystems, 6(2), 114–128, doi:10.1007/s10021-002-0121-9, 2003.

Larcher, W.: Ökophysiologie der Pflanzen, UTB, 394, 1994.

Molto, Q., Hérault, B., Boreux, J.-J., Daullet, M., Rousteau, A. and Rossi, V.: Predicting tree heights for biomass estimates in tropical forests - a test from French Guiana, Biogeosciences, 11(12), 3121–3130, doi:10.5194/bg-11-3121-2014, 2014a.

Molto, Q., Hérault, B., Boreux, J. J., Daullet, M., Rousteau, A. and Rossi, V.: Supplement of: Predicting tree heights for biomass estimates in tropical forests -A test from French Guiana, Biogeosciences, 11(12), 3121–3130, doi:10.5194/bg-11-3121-2014, 2014b.

Myneni, R., Knyazikhin, Y. and Park, T.: MODIS/Terra+Aqua Leaf Area Index/FPAR 8-day L4 Global 500m SIN Grid V006, NASA EOSDIS L. Process. DAAC, doi:doi.org/10.5067/MODIS/MCD15A2H.006, 2015.

R Core Team: R: A Language and Environment for Statistical Computing, [online] Available from: https://www.r-project.org/, 2019.

Robinson, D. and Hayes, A.: broom: Convert Statistical Analysis Objects into Tidy Tibbles, [online] Available from: https://cran.r-project.org/package=broom, 2020.

Rutishauser, E., Wagner, F., Herault, B., Nicolini, E.-A. and Blanc, L.: Contrasting above-ground biomass balance in a Neotropical rain forest, J. Veg. Sci., 21(4), 672–682, doi:10.1111/j.1654-1103.2010.01175.x, 2010.

Ryan, M. G.: Effects of Climate Change on Plant Respiration, Ecol. Appl., 1(2), 157–167, doi:10.2307/1941808, 1991.

Simard, M., Pinto, N., Fisher, J. B. and Baccini, A.: Mapping forest canopy height globally with spaceborne lidar, J. Geophys. Res., 116(G4), G04021, doi:10.1029/2011JG001708, 2011.

Wickham, H., Averick, M., Bryan, J., Chang, W., McGowan, L. D., François, R., Grolemund, G., Hayes, A., Henry, L., Hester, J., Kuhn, M., Pedersen, T. L., Miller, E., Bache, S. M., Müller, K., Ooms, J., Robinson, D., Seidel, D. P., Spinu, V., Takahashi, K., Vaughan, D., Wilke, C., Woo, K. and Yutani, H.: Welcome to the {tidyverse}, J. Open Source Softw., 4(43), 1686, doi:10.21105/joss.01686, 2019.

Zanne, A. E., Lopez-Gonzalez, G., Coomes, D. A. A., Ilic, J., Jansen, S., Lewis, S. L. S. L., Miller, R. B. B., Swenson, N. G. G., Wiemann, M. C. C. and Chave, J.: Data from: Towards a worldwide wood economics spectrum. Dryad Digital Repository., 2009.